J Comp Physiol A (1988) 163:201–213

Journal of Comparative Physiology A Sensory, Neural, and Behavioral Physiology

Visual optics in toads (*Bufo americanus*)

Ute Mathis, Frank Schaeffel, and Howard C. Howland*
Section of Neurobiology and Behavior, Cornell University, Ithaca, New York 14853, USA

Accepted January 4, 1988

Summary. Aspects of visual optics were investigated in the American toad (*Bufo americanus*). The development of the refractive state of the eye during metamorphosis was followed with IR photoretinoscopy. Frozen sections documented the changes in optical parameters before and after metamorphosis. There is a difference in light sensitivity between juvenile and adult toads. Binocular accommodation in adult toads was observed.

1. IR photoretinoscopic measurements showed that the refractive state of the eye changed very rapidly during metamorphosis, about 10 *D*/h while the animal entered the terrestrial habitat.

2. Frozen sections showed that the almost spherical lens in a tadpole eye had flattened in a just metamorphosed toad's eye while at the same time the distance of the lens to the retina had decreased. However, the morphological measurements were not sufficiently sensitive to record the relatively small changes in ocular dimensions that were responsible for the rapid changes in refractive state during metamorphosis.

3. Schematic eyes, with homogeneous and non homogeneous lenses, were constructed for tadpoles, juvenile toads, and adult toads.

4. Nonparaxial raytracing studies in schematic eyes suggested that the lenses of animals of the three developmental stages tadpole, juvenile toad, and adult are not homogeneous but have a refractive index gradient. The raytracing studies indicated that the refractive index gradient is different for the different developmental stages, being highest in the tadpole lens.

5. The observations of toads during feeding behavior at different light levels showed an increased light sensitivity in the adult nocturnal toads in contrast to the juvenile animals, which are diurnal. The increased light sensitivity could partly be explained with an increase in aperture and an increase in red rod outer segments. To fully explain the higher light sensitivity in adult toads, changes in neuronal parameters had to be assumed.

6. Retinoscopic measurements of the resting refractive state in the adult toad showed a hyperopic defocus of about +8 *D*. By subtracting the measurement artefact for retinoscopy, the true resting focus was found to be nearly emmetropic.

7. The amount of natural accommodation in adult toads during normal feeding behavior was investigated with IR photoretinoscopy. Binocular accommodation of about 8 *D* was observed.

Introduction

Amphibians mark the evolutionary transition from aquatic to terrestrial life. They undergo metamorphosis during their development. During metamorphosis the amphibian eye has to correct for changes in refractive power of the cornea due to environmental changes from water to air. Duke-Elder (1958) indicated that differences in shape and position of the lens are responsible for these corrections. Sivak and Warburg (1980) confirmed these observations for the metamorphosis of *Salamandra salamandra*. Using infrared photoretinoscopy we observed changes of the refractive state before, during, and after metamorphosis in the American toad (*Bufo americanus*). At the same time frozen sections of toads of different developmental stages were measured to show simultaneous changes in optical parameters in the eye. In addition, we constructed schematic eyes for different developmental stages to give a more accurate description of the

Abbreviations: *D* Diopter; *IR* infrared light; *LED* light emitting diode; *ROS* red rod outer segments; *SF* shape factor

* To whom correspondence should be addressed

changes occurring in the amphibian eye during development.

Field studies suggested that small, just metamorphosed toads are diurnal, unlike adult which are nocturnal (Eibl-Eibesfeldt 1967; Taigen and Pough 1981). Larsen and Pederson (1982) found that adult toads were able to snap towards mealworm dummies at a light level of only 30 μLux. We were interested to determine whether the eyes of adult toads, when compared to those of juveniles, show special adaptations to this increased light sensitivity.

In addition we investigated the accommodative ability of toads during feeding behavior. Anurans are thought to accommodate by changing the position of the lens with the aid of two protractor lentis muscles (Beer 1898; Hess 1911; Tretjakoff 1913). It has been suggested (Ingle 1968, 1976; Collett 1977; Jordan et al. 1980) that in monocular anurans the accommodative state in the eye plays a role in estimating the distance to the prey during feeding behavior. Douglas et al. (1986) were able to produce binocular accommodation of about 10 *D* in toads (*Bufo viridis*) by applying drugs. Their measurements are in agreement with the idea that accommodation is achieved by moving the lens and not by changing the shape of the lens or the cornea. We used infrared photoretinoscopy to measure the natural refractive state in the American toad both at rest and during feeding behavior.

Materials and methods

Animals

All observations were made on specimens of *Bufo americanus*. Metamorphosis is defined as the moment when the aquatic tadpoles leave water and become terrestrial toads. In most cases the age of toads after metamorphosis was known. If the age was not known, it was estimated by measuring body length and checking for the presence of a tadpole tail, which is lost within 1–2 days after metamorphosis.

Eye changes during metamorphosis

Refractions. IR light, produced by high output IR LED's, provides three advantages over normal photoretinoscopy: (1) there is no light induced pupillary constriction, (2) the animal is not aware of the fact that it is being measured and (3) the measurements can be performed in complete darkness. The optical basis of photoretinoscopy is given in Fig. 1. An LED centered in the video camera aperture will be imaged on the retina. Light returning from the fundus will be refocused on the LED itself by the optical system of the eye (eye focused on LED) or it will be spread out into a cone (eye defocused with respect to the camera). For an eye with high optical quality, light will be seen in the pupil only in the latter case. When a black paper shield is positioned behind the LED, (1) a certain amount of defocus is necessary for a light reflex to be seen in the pupil at all and (2) the sign of defocus can be determined from the position of the fundus reflex in the pupil (myopic: bottom of the pupil; hyperopic: top of the pupil). The measurement range can be greatly extended by positioning light sources (LED's) at different distances, or eccentricities, from the edge of the paper shield. Whether or not a reflex can be detected depends on the defocus of the eye relative to the camera plane (*D*), the pupil radius (*R*), the eccentricity (*E*) of the LED from the optical axis of the video camera, and the distance between the recorded eye and the camera (*A*). Using raytracing techniques in a theoretical treatment of photoretinoscopy by Howland (1985), the defocus of the eye was shown to be given by the formula

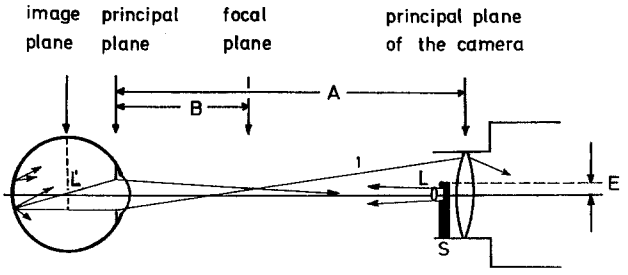

Fig. 1. Optics of photoretinoscopy. In a myopic eye (focal plane at *B*) a real image of the light source, *L*, is formed at *L'* in front of the retina, whereas a blurred spot appears on the retina. Light reflected from the fundus leaves the eye through the pupil and is refocused in the focal plane of the eye, *B*, between the eye and the camera; it diverges subsequently. If the lower part of the camera aperture is occluded by a black paper shield, *S*, only rays emerging from the bottom of the pupil, such as *1*, are detected by the unvignetted part of the aperture and recorded by the camera. The distance of the light source from the upper margin of the paper shield represents the eccentricity *E*. The LED must not necessarily be centered at the optical axis; the critical parameter for determining the defocus is only the distance of the LED to the edge of the paper shield.

$$D=\frac{E}{2A^{*}DF^{*}R} \quad (1)$$

where *DF* is the dark fraction or ratio of the portion of the diameter of the pupil which is dark to that which is illuminated by the fundus reflex.

A computer program allowed us to store several consecutive video frames while LED's at different eccentricities were flashed in sequence. Photographs documenting the measurements were then taken from the video screen. For further information on this method, see Schaeffel and Howland (1987). The appearance of the fundus reflex in the pupil during IR photoretinoscopy gives an estimate for the spherical abberration present in the eye. In a high optical quality eye the fundus reflex in the pupil appears as a crescent with a straight edge towards the center of the pupil. If, however, spherical aberration is present, the central edge of the reflex crescent becomes concave or convex depending on whether the aberration is positive or negative. In a myopic eye, positive aberration shows up as a concave crescent. By contrast, for a hyperopic reflex, the central edge would be convex. The difference in the calculated refractive state of the eye, computed from the reflex segment height in the center and in the margin of the pupil, gives an estimate of the amout of spherical aberration.

Photokeratometry. The corneal radius of curvature was measured by a large IR photokeratometer. The first Purkinje images of 8 IR LED's arranged in a circle with a radius of 149 mm were evaluated in a highly magnified (35 μm per pixel) video

image. A computer program was used to detect the position of the Purkinje images in the digitized video frame. The same program calculated the corneal radius of curvature from the diagonal distance of the light dots (Schaeffel and Howland 1987). The arrangement was calibrated using a series of ball bearings of known radius of curvature. The accuracy of the procedure is $\pm 1\%$. Using this technique, only the corneal radius of curvature of adult toads could be measured. The eyes of the juvenile toads were too small to be measured accurately.

Measurements of ocular dimensions in frozen sections and raytracing studies on schematic eyes. Adult animals were sacrificed by decapitation. Tadpoles and juvenile toads had to be anesthetized prior to decapitation. In each case the head was immediately frozen in an embedding medium (Tissue-Tek) and then placed on the plate of a freezing microtome. The head was sectioned down to the plane of the estimated largest diameter. Several photographs were taken of the remaining block of tissue, using a Nikon camera equipped with a macrolens. Sections through the central portions of the globes were 8 µm apart. According to Sivak and Warburg (1980), photographs of sections showing maximum thickness of the lens were assumed to represent horizontal sections through the geometrical axis of the eye. In contrast to standard histological sections, this technique minimizes distortion of ocular shape. Intraocular distances and curvatures were measured on highly enlarged (about 25×) photographic prints. Curvatures (r) were calculated from the formula

$$r=(y)^2/2s+s/2 \quad (2)$$

where y is 1/2 of the chord of a curved surface that is assumed to be spherical and s is the sagittal depth of that chord (Sivak and Warburg 1980). Except for corneal radius of curvature in the live adult toads, radii were obtained from frozen sections.

Nonparaxial raytracing of schematic eyes was performed. In contrast to paraxial raytracing, this approach allows one to study spherical aberration in lenses with refractive index gradients. The refractive state of the schematic eye varies with the distance of the ray to the optical axis. The maximum difference in refractive state calculated from rays with different distances to the optical axis gives an estimate for the amout of spherical aberration present in the eye. Another advantage of nonparaxial raytracing is that the refractive state in the peripheral visual field can be examined for a particular lens model. We employed a computer program that uses spherical approximations of intraocular surfaces. In our model spherical aberration could be minimized by placing onion shaped shells ($n=100$) of adjustable shape into the lens, thereby simulating a continuous gradient lens. The index increased in equal steps from the margin to the center of the lens. A shape factor (SF) allowed us to continuously vary the shape of the interior shells in the lens between two extreme positions. Either the radii of curvature of the interior shells were kept constant while the centers of curvature were moved along the optical axis (SF = 0, Fig. 2A) or the centers of curvature were kept at a fixed position while the radii decreased concentrically (SF = 1, Fig. 2C). In all cases the radii of curvature of the external surfaces of the lens were kept constant and identical to those of the non-shelled model. Shapes and positions of shell segments in the anterior and posterior part of the lens were calculated separately. Intersections between both segments had to be calculated for every individual shell in order to assure that iso-indicial surfaces were closed. For intermediate values of SF between 1 and 0 (for example SF = 0.6, Fig. 2B) combined changes in radii and positions were produced:

$$S\,(\text{position})=(1-\text{SF})^{*}d/(n+1) \text{ and} \quad (3)$$

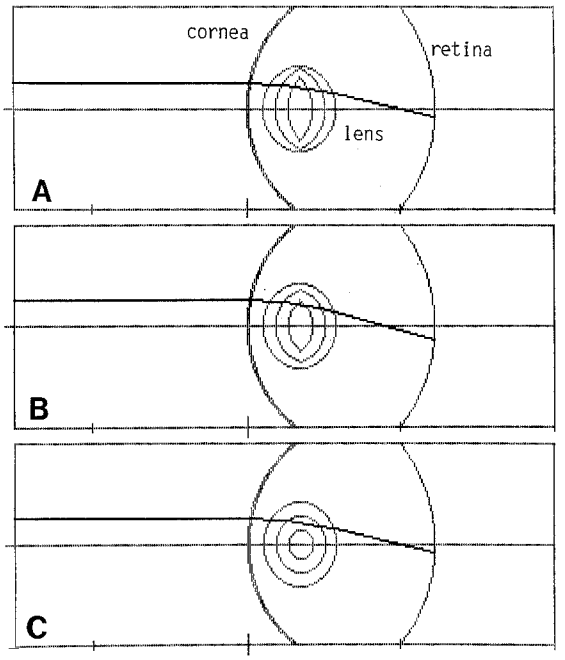

Fig. 2A–C. Models for a gradient lens (which for illustrative purpose contains only 3 shells) with different shape factors. **A** Shape factor (SF) 0; **B** shape factor (SF) 0.6; **C** shape factor (SF) 1. Note that when the shape factor is 0 the radii of curvature of the interior shells were kept constant while the centers of curvature were moved along the optical axis and that when the shape factor is 1 the centers of curvature were kept at a fixed position while the radii decreased concentrically

$$S\,(\text{radius})=\text{SF}^{*}d/(n+1) \quad (4)$$

where S (position) and S (radius) are the stepsizes between individual shells, d is the height of the respective lens segment (either anterior or posterior), and n is the number of shells. For refractive indices we used values given for the frog eye (*Rana esculenta*) by du Pont and de Groot (1976): cornea ($n=1.39$), fluid of anterior chamber ($n=1.338$), and vitreous body ($n=1.338$). We also used the value of $n=1.65$ for the homogeneous (non-shelled) lens. In our gradient index lens model (shelled), we used a uniform refractive index gradient and adjusted the limits of this gradient and the shape factor, while holding the outer radii of curvature and the position of the lens constant, until the focus and spherical aberration of the eye matched our photoretinoscopic observation.

Light sensitivity of juvenile and adult toads

Effect of different light levels on the first attention distance during feeding behavior. Feeding behavior of adult and juvenile toads (1–2 weeks after metamorphosis) was recorded at different light intensities with an infrared video camera. For illumination we used tungsten light bulbs with a color temperature of 3200 K. Light intensity was measured with a luxmeter (Tektronix J16) with a threshold sensitivity of 0.01 Lux. After a 40 min period of adaptation to the respective light level, the toads were placed into a container that had its bottom covered with graph paper. For adult toads the squares on the paper were 5 cm and for juvenile toads the squares were 1 cm. With the aid of this grid, the distance between the toad and the prey (mealworms for adult toads and fruit flies for juvenile toads) was measured as the toad turned towards the prey for the first time. This

distance is referred to as the first attention distance. We evaluated only those observations where the first attention, developed independently from the behavior of other toads, was followed by an active tracking and a successful capture of the prey. From the first attention distance and the length of the prey (mealworms: 20 mm; fruit flies: 3.4 mm), we calculated the visual angle.

Measurements of f-number. The *f*-number (the ratio of posterior nodal distance to pupil diameter) gives an estimate of the brightness of the retinal image which is proportional to $1/(f\text{-number})^2$. We shone IR light into dark adapted toad eyes and measured the diameter of the pupils so illuminated. The posterior nodal distances were obtained from the schematic eyes (see Table 3).

Measurements of photoreceptor dimensions. In a light adapted retina the expanded pigment epithelium obscures the photoreceptors. Accordingly each animal was dark-adapted for 40 min, then decapitated (adults) or anesthetized and decapitated (juveniles). After dehydration in graded percentages of alcohol and clearing in xylene the entire heads of juvenile toads were embedded in Paraplast. For adult animals, only dissected eyeballs were embedded. The eyes were vertically sectioned with a microtome and the 7 µm thick sections were stained using Mallory Heidenhain Azan Stain (Koneff 1938). Sections were photographed under the light microscope at objective magnifications of 40× and 100× (oil).

According to Tsukamoto (1987), the length and width of rod outer segments vary depending on their location in the retina of bullfrogs (*Rana catesbeiana*). Therefore, we measured the length and the width of red rod outer and inner segments at the dorso-central retina near the optic disc where they are greater in length, smaller in cross-sectional area, and higher in density. Within this area we measured only red rods with a clear-cut structure. Red rods can easily be distinguished from green rods by their longer outer and shorter inner segments. Morphological measurements were carried out on the light microscope with the aid of a micrometer disc reticle (10 mm/100 per Division). All data are presented with no correction for shrinkage.

Accommodation during feeding behavior in adult toads

Toads were maintained under a natural light cycle. While adult toads were feeding, we measured the refractive state of their eyes using IR photoretinoscopy. All measurements were taken under dim light during early night hours (6 pm–10 pm) when the nocturnal toads showed increased activity. The toads were placed into a glass terrarium where a small area was separated by a plexiglas pane. We placed mealworms as prey objects into the separated area. The toads could track the moving mealworms with their eyes but could not actively pursue and catch them. The refractive state was recorded continuously with IR photoretinoscopy. Each experiment was limited to 5–10 min to prevent fatigue in the animal. After the experiment, the toad was always rewarded with a mealworm.

Results

Eye changes during metamorphosis

Changes in refractive state. We followed the refractive state of toad eyes during metamorphosis as measured by IR photoretinoscopy in air (Fig. 3).

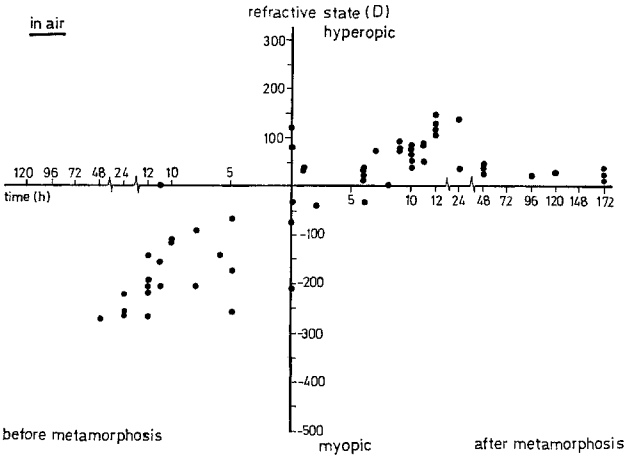

Fig. 3. Development of the refractive state during metamorphosis as measured with IR photoretinoscopy (in air). Note that tadpoles are strongly myopic in air shortly before metamorphosis (−275 *D* maximum). The eyes become emmetropic or hyperopic within a few hours after entering the terrestrial habitat. Data from 24 individuals. Note breaks in horizontal scale

When measured in air, tadpoles are strongly myopic (−275 *D* maximum) 1–2 days before metamorphosis. When measured in water, they appear to be hyperopic. Tadpoles of earlier developmental stages appear to be myopic (−30 *D*) when measured in water. During metamorphosis the focus changes about 10 *D* per hour with the slope of the regression line: y (Diopters) $= -47.07 + 11.588\times$ (hours). At metamorphosis there are myopic (see Fig. 4A), emmetropic (see Fig. 4B), and hyperopic (see Fig. 4C) individuals. We never saw a toad that was still myopic in air more than 8 h after metamorphosis. High levels of hyperopia are measured until about 12 h after metamorphosis. The hyperopia then gradually declines over the next few weeks. The refractive change can be attributed to the diminishing small eye artefact of retinoscopy (Glickstein and Millodot 1970). After metamorphosis the eye grows rapidly, and the thickness of the retina relative to the total eye size decreases, thereby decreasing the seeming hyperopic defocus.

Changes of ocular dimensions as measured in frozen sections and raytracing studies on schematic eyes. In accordance with the data from *Salamandra salamandra* (Sivak and Warburg 1980), it was found that the lens in the tadpole (see Fig. 5A) is almost spherical, as is characteristic for aquatic animals. In juvenile toads 2 weeks after metamorphosis (see Fig. 5B), the lens has already flattened and has moved posteriorly, thereby decreasing its distance from the retina. Both effects result in a decrease

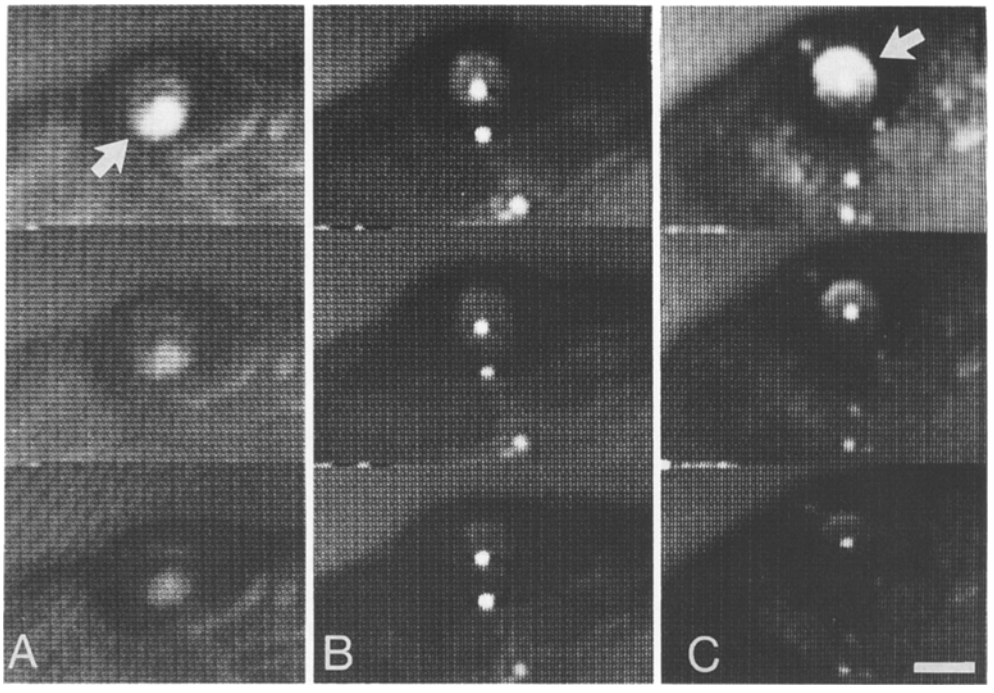

Fig. 4A–C. IR photorefractions of toads of different development stages. In each case 3 consecutive measurements were taken within about 500 ms while IR light sources of increasing eccentricities were flashed into the eye. (bar represents 1 mm) **A** Myopic reflex in a tadpole's eye just at metamorphosis (in air). Note the fundus reflex at the bottom of the pupil. **B** Emmetropic refraction of a tadpole just at metamorphosis (in air). **C** Hyperopic reflex (top of pupil) in the eye of a just metamorphosed toad (in air)

of the refractive power of the eye. The relative thickness of the retina is much greater in a juvenile toad eye (see Fig. 5B) than in an adult toad (see Fig. 5C) although the absolute thickness remains about constant. This observation is consistent with our retinoscopic measurements, which indicated a much smaller amount of hyperopia (+8 *D*) in the adult toad. We interpret this hyperopia to be small eye hyperopia. The frozen sections also indicate that the axis of both eyes converge during ontogeny as described in *Salamandra salamandra* (Sivak and Warburg 1980).

Adult toad

With data (see Table 1) obtained from frozen sections, we constructed a schematic eye for the adult toad (see Fig. 6C, Table 2 and Table 3). Measurements of the refractive index of the frog (*Rana esculenta*) lens (du Pont and de Groot 1976) indicate that the lens is not homogeneous but that the index is highest in the core: 1.47, diminishing to 1.39 at the margin. Du Pont and de Groot did not use these values directly for computation. Instead they found their schematic eyes to be in focus with a lens index of 1.65, using a homogeneous lens model. If we apply their refractive index to our schematic eye, we get a highly myopic defocus and certainly a high level of spherical aberration. By diminishing the refractive index to 1.566 and taking the vitreoretinal interface as the image plane, the hyperopic defocus of +8 *D* matches the retinoscopically measured defocus (+8 *D*). But spherical aberrations of 61 *D* (for a pupil radius of 1.5 mm) are much too high and are not consistent with spherical aberrations of about 2 *D* as estimated from the appearance of the fundus reflex in the pupil during IR photoretinoscopy. By testing several models of gradient lenses, in which the outer radii of curvature and position of the lens were kept constant, we found that a gradient lens (100 shells, SF = 0.6) with a core index of 1.5 and a marginal index of 1.375 gave the best results. The refractive state was +9 *D* (hyperopic), and the longitudinal spherical aberration was 4 *D* (pupil radius = 1.5 mm). By moving the image plane from the interface layer between retina and vitreous to the photoreceptor layer a difference of about 200 μm we reduced the defocus to about 0 *D*. The hyperopia measured retinoscopically (about 8 *D*) comes close to the calculated small eye artefact (9 *D*). For the schematic eye given above, the refractive state stays about constant up to 20 deg off-axis.

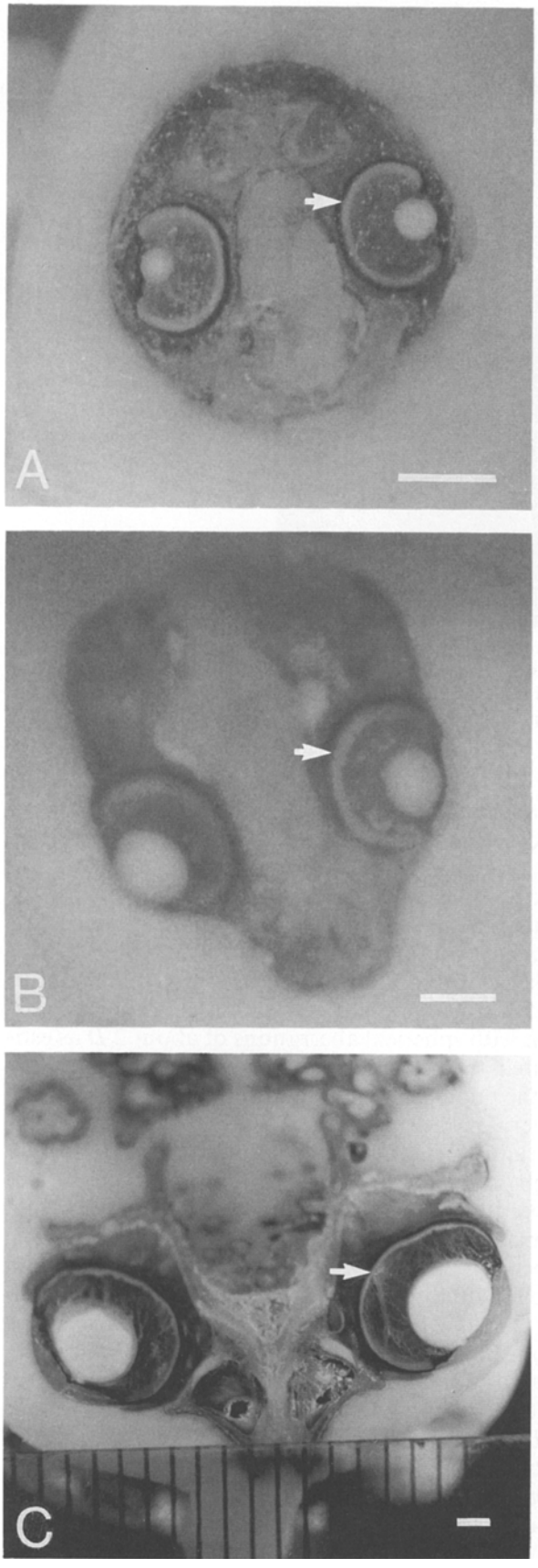

Juvenile toad and tadpole

Figure 6A, B shows schematic eyes for the tadpole and just metamorphosed toad. Tables 1, 2, and 3 give the corresponding ocular parameters. If we apply the model of a homogeneous lens to the schematic eyes of juvenile toads and tadpoles, we must use different refractive indices to match the retinoscopically measured mean refraction which is for the juvenile toad 1 week after metamorphosis (in air): +35 *D* hyperopic, $n=3$; for the tadpole (in water): −30 *D* myopic, $n=3$. In the tadpole eye a homogeneous lens index of 1.6105 produces the observed myopic defocus (see Table 3), whereas in the juvenile toad, a slightly lower refractive index ($n=1.575$) is necessary to give the measured hyperopic defocus of +35 *D* (see Table 3). But in both cases, spherical aberration is much too high (tadpole: 395 *D*; juvenile toad: 238 *D*) and does not agree with estimations of spherical aberration made from the appearance of the fundus reflex during photoretinoscopy, which was about 30 *D* for both tadpole and juvenile toad. By testing several different index gradients for the juvenile toad lens while keeping the outer radii of curvature and the position of the lens constant, we found that a gradient lens (100 shells) with a shape factor of 0.7 and refractive indices of 1.34 (margin) and 1.5 (core) gave a hyperopic defocus of +37 *D*, close to the retinoscopically measured mean defocus of +35 *D*. At the same time, spherical aberration in the juvenile toad eye could be reduced to about 21 *D*. In the tadpole eye we had to use a slightly steeper gradient in the lens ($n=1.33$ [margin] and $n=1.5$ [core]) than in the juvenile toad to match the observed myopic defocus of −30 *D* (in water). The lowest amount of spherical aberration (60 *D*) was produced for a shape factor of 0.428. Spherical aberration could not be further reduced with the degrees of freedom given by our model.

The calculated small eye artefact for a tadpole eye was about 350 *D* and, for the eye in a juvenile toad, about 130 *D*.

Fig. 5A–C. Frozen sections of heads of a tadpole, a juvenile and an adult toad. Arrows indicate always the position of the retina. **A** Frozen section through a tadpole head in the horizontal plane (bar represents 1 mm). Note the spherical shape of the lens and the large distance from lens to retina. **B** Frozen section of a small toad, 2 weeks after metamorphosis (bar: 1 mm). The refractive state in air was about +30 *D* (hyperopic). Note that the lens has flattened and that the distance to the retina has decreased. **C** Frozen section of the head of an adult toad (bar: 1 mm). The refractive state was about +8 *D* (hyperopic). The relative thickness of the retina is much smaller if compared to the retina in Fig. 5B. Accordingly the small eye artefact of retinoscopy is less prominent

Table 1. Mean positions and radii of curvature of optical surfaces (mm)

	Cornea ant.	Cornea post.	Lens ant.	Lens post.	Retina ant.[a]	Photorec. layer
Tadpole ($n=5$)						
Position	0	0.020	0.114	0.581	1.072	1.222
Radius	0.717	0.697	0.240	−0.253	−0.752	−0.864
Juv. toad ($n=5$)						
Position	0	0.020	0.229	0.845	1.420	1.620
Radius	0.734	0.714	0.501	−0.366	−0.765	−0.990
Adult toad ($n=3$)						
Position	0	0.200	0.782	3.590	5.899	6.099
Radius	2.564	2.364	2.339	−1.785	−2.975	−3.128

[a] The anterior surface of the retina is equivalent to the vitreoretinal interface. Standard deviations for positions of optical surfaces ranged from 20–25 μm and for radii of curvature of optical surfaces from 20–30 μm

Table 2. Lens models and refractive indices

	Lens (refract. index)	Number of shells	Shape factor
Tadpole			
Paraxial model	1.6105	0	none
Non paraxial model	1.33–1.5	100	0.428
Juv. toad			
Paraxial model	1.575	0	none
Non paraxial model	1.34–1.5	100	0.7
Adult toad			
Paraxial model	1.566	0	none
Non paraxial model	1.375–1.5	100	0.6

For refractive indices of the other optical surfaces we used values given for the frog eye (*Rana esculenta*) by du Pont and de Groot (1976): cornea ($n=1.39$), fluid of anterior chamber ($n=1.338$), vitreous body ($n=1.338$)

Table 3. Cardinal points for Gaussian approximation (paraxial eye model)

	Tadpole	Juv. toad	Adult toad
Total refract. power (D)	1842	1218	284
Ant. focal length (mm)	−0.543	−0.821	−3.524
Post. focal length (mm)	0.726	1.098	4.714
Ant. princip. point (mm)	0.216	0.331	1.209
Post. princip. point (mm)	0.256	0.382	1.369
Ant. nodal point (mm)	0.400	0.608	2.400
Post. nodal point (mm)	0.440	0.659	2.560
Refraction[a]	−30.2	+35.0	+8.3

[a] Refraction (with respect to vitreoretinal interface) in air for juvenile and adult toad and in water for tadpole; negative sign indicates a myopic refraction relative to infinity, a positive sign a hyperopic refraction

Changes in light sensitivity from the juvenile toad to the adult toad

Effect of different light levels on the first attention distance during feeding behavior. For juvenile toads 1–2 weeks after metamorphosis, we chose light intensities of 18 Lux, 6.1 Lux, and 0.48 Lux. Below 0.48 Lux the juvenile toads were not active at all. In Fig. 7A one can see that with decreasing light intensity, the mean visual angle subtended by the prey object at the first attention distance increases significantly. From $a=12.5$ at 6.1 Lux to $a=17.2$ at 0.48 Lux, df=54, $t=2.3$, $P<0.02$. From $a=9.4$ at 18 Lux to $a=17.2$ at 0.48 Lux, df=53, $t=4.6$, $P<0.001$ (Student's t-test). In other words, with decreasing light levels the toad has to be closer to the prey to display orientation behavior. Figure 7B shows the analogous measurements for adult toads. We had to choose lower luminances of 6.1 Lux, 0.41 Lux and 0.02 Lux because the nocturnal adult toads were inactive at the highest light level used in Fig. 7A. There was no significant change in the mean visual angle (a) while light levels were lowered (6.1 Lux, $a=5{,}3$; 0.41 Lux, $a=4.9$; 0.02 Lux, $a=5.3$; n.s.). Apparently, the tested light levels were not critical for feeding in adult animals.

Changes in optical parameters and photoreceptor dimensions

Based on frozen sections and measurements of the pupil size in living animals, we determined the f-number of eyes. The adult animals show a mean f-number of $f=0.85$ (± 0.19, $n=3$) versus $f=1.58$ (± 0.18, $n=4$) in juvenile toads (df=5, $t=5.14$, $P<0.005$; Student's t-test). The smaller f-number in adult toads is equivalent to an increase in retinal illumination of about 3.5 times. However, the difference in the f-number is not sufficient to explain

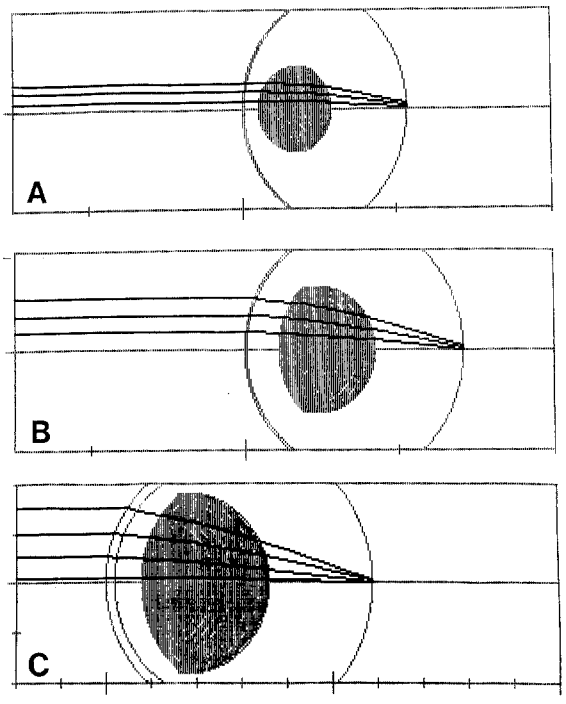

Fig. 6A–C. Schematic eyes for different developmental stages of toads. All 3 eyes have a gradient lens (100 shells, SF=0.6) with a core index of 1.5 and a marginal index of 1.375. For positions and radii of curvatures in the schematic eyes see Tables 1 and 2. For refractive indices of optical surfaces see Table 3. **A** Schematic eye of a tadpole; **B** Schematic eye of a toad 1–2 weeks after metamorphosis; **C** Schematic eye of an adult toad

the behaviorally measured increase in light sensitivity which is about 20 times higher in adult toads than in juvenile toads. Other parameters must also have changed.

According to Walls (1942), there are 4 different types of photoreceptors in the amphibian retina: violet (red) and green rods, single and double cones. The green rod is found only in amphibians among which it is widely distributed. Its outer segment is short and its inner segment long and thin in contrast to the red rod where the outer segment is long and the inner segment is short. In structure, therefore, it occupies an intermediate position between a cone and an ordinary (red) rod (Walls 1942). Absorption maxima for the red and green rods are 502 nm and 432 nm, respectively (Gordon and Hood 1976). Figure 8 shows the length/width ratio for red rod inner and outer segments for different developmental stages. Within one week before metamorphosis and the first 6 weeks after metamorphosis, there is no significant change in the ratio of length to width, neither for the outer nor the inner segments.

However, the red rod outer segments are significantly longer in adult toads than in toads of earlier developmental stages, while the width does not change (see Figs. 8 and 9A, B). For the inner segments there is no difference between the length/width ratios in adult and juvenile toads.

These results can help explain the observations made during feeding at different light levels. The lengthening of the outer segments seen in adult animals, which contributes to an increased light sensitivity, must happen later during development. Furthermore it appears to be a continuous process, since it is also documented in the difference in the ratio of length to width of rod outer segments between the 2 year old and 4 year old toad.

Binocular accommodation during feeding behavior in adult toads

The resting refractive state in the adult toad eye as measured with IR photoretinoscopy is about +8 *D* (hyperopic) (see Fig. 10A). For comparison, conventional streak retinoscopy was performed and gave similar results of a resting refractive state of +7 *D* hyperopic. We recorded the refractive state of the eyes of adult animals during feeding behavior with IR photoretinoscopy. As soon as the toad detected the mealworm, it pursued it visually and moved back and forth in front of the plexiglas pane to catch it. If the mealworm came into the critical snapping distance, determined by the length of the toad's tongue, the toad fixated the prey object for some seconds. Then, just prior to snapping, it changed the refractive state of the eyes. The hyperopic reflex crescent in the pupil disappeared, which is equivalent to about 8 *D* of accommodation (see Fig. 10B). Accommodation took place in both eyes simultaneously. The focus changed within about half a second and was strictly related to feeding.

We could never induce any changes in refractive state by presenting artificial targets. There was no obvious near-pupillary reflex (Davson 1984). The optical quality, as evaluated from the appearance of the photoretinoscopic reflex in IR light was not very good during accommodation because hyperopic and myopic reflex crescents appeared simultaneously (see Fig. 10B). Such an event is unlikely to be due to chromatic aberration since this type of aberration is greatly reduced in the infrared. Furthermore accommodation was not necessary for the toad to catch the prey. After the plexiglas pane had been removed, we observed successful snapping responses when no accommodation had taken place.

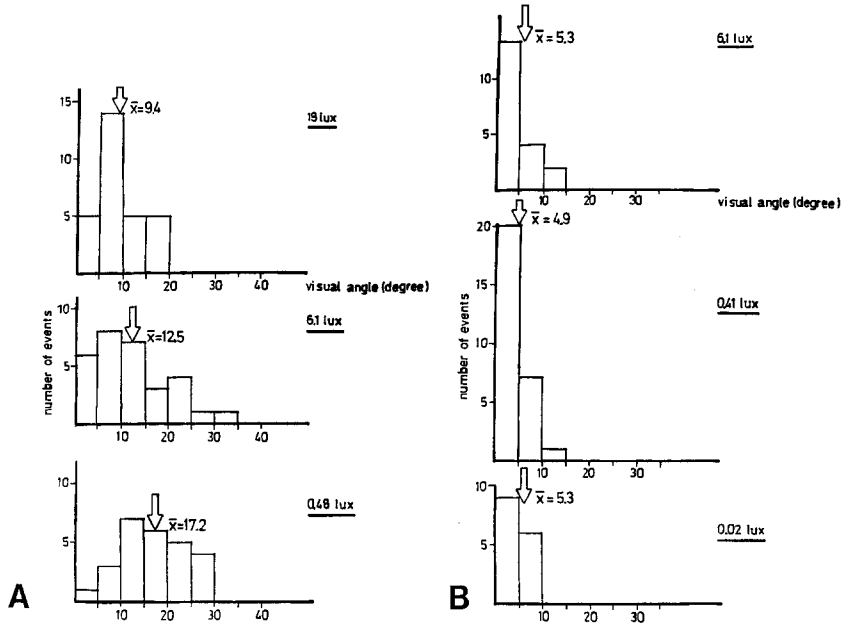

Fig. 7 A, B. Visual angle (deg) subtended by a prey object at the distance that first elicited orientation behavior. **A** In small toads (1–2 weeks old) one can see that with decreasing light intensities (18 Lux, 6.1 Lux and 0.48 Lux) the visual angle increases significantly. In other words the toad has to be closer to the object in order to show orientation behavior. **B** Analogous measurements for adult toads. Lower luminances were chosen (6.1 Lux, 0.41 Lux and 0.02 Lux) because adult toads were inactive at the highest light level chosen in **A**

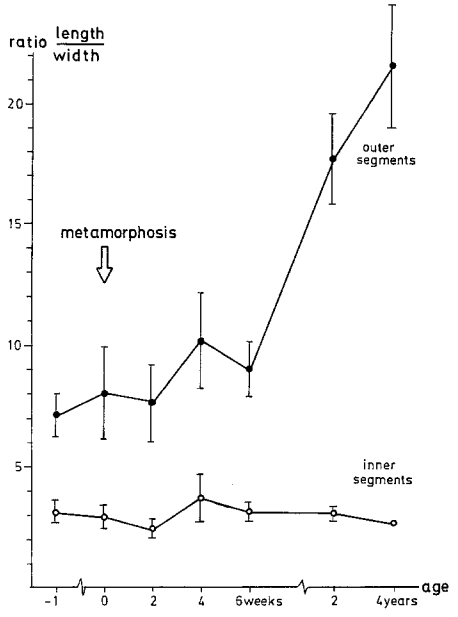

Fig. 8. Length (μm)/width (μm) ratio of red rod outer and inner segments as a function of age (metamorphosis is defined as time zero). Each point represents the mean value with standard deviation of 3 to 5 individuals

Discussion

Eye changes during metamorphosis

As stated earlier, the results of retinoscopy are strongly influenced by the small eye artefact wherein the reflecting layer is not identical with image plane. We computed the magnitude of this artificial defocus due to the small eye artefact based on the assumption that there is only one distinct reflecting layer at the vitreoretinal interface with no intermediate position. However, the small eye artefact is not responsible for the observed changes in refractive state during metamorphosis. Like Sivak and Warburg (1980), we found that there appears to be little difference in retinal thickness between eyes from stages just before and just after metamorphosis. Also the axial length of the eye in tadpoles of late developmental stages is not significantly different from that of just metamorphosed toads.

The retinoscopic measurements show that tadpoles of early developmental stages are myopic if measured in water. This finding is consistent with investigations of Manteuffel et al. (1977) where measurements of the refractive state of larval forms of *Salamandra salamandra* with the laser speckle method showed a myopic defocus of about $-3\ D$ in water. Considering the small eye artefact, which is present in both methods, we can assume that tadpoles of early developmental stages (and *Salamandra salamandra* larvae) are much more myopic in water. When the tadpoles approached metamorphosis, measurements of the refractive state showed a hyperopic defocus in water. If measured in air they appear to be extremely myopic. The large amount of myopia in air is due to the additional refractive power of the cornea which is lost in vision underwater. The difference in refractive power between vision in air and underwater can be calculated from the corneal radius of curvature

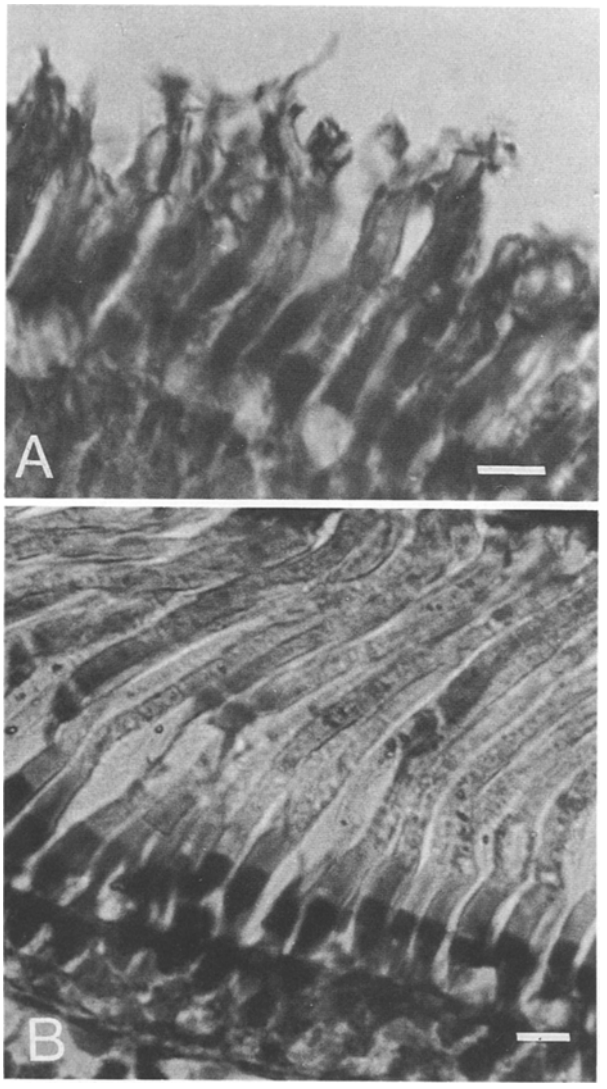

Fig. 9A, B. Light micrographs of red rods in vertical section (bar indicates 5 μm). **A** Red rods in the retina of a toad 2 days after metamorphosis. **B** Red rods in the retina of an adult toad (4 years old)

of the metamorphosing toad; it is about 400 *D*. Frozen sections of a tadpole head before metamorphosis showed the optical parameters that contribute to the strong refractive power of the larval eye: a strongly curved, almost spherical lens and a relatively large distance between lens and retina. As seen from our retinoscopic measurements, during metamorphosis the refractive state changes rapidly, within hours. Frozen sections of heads from tadpoles at different stages of metamorphosis didn't reveal a sudden change in shape and position of the lens. However, such changes in ocular dimensions were present on frozen sections of toads 1–2 weeks after metamorphosis. The changes in ocular dimensions in frozen sections, which are responsible for the rapid changes in refractive state during metamorphosis, are relatively small. Computations that take into consideration the possible reading error for radii of curvature and lens position show that our morphological measurements are not sufficiently sensitive to record these small changes.

During development, morphological differentiation of the amphibian lens into the primary fiber cells of the nucleus and the secondary fibers of the cortex is accompanied by a change in soluble lens protein (Doyle and Maclean 1978). Gamma crystallin is the earliest detectable embryonic lens protein. Brahma and Bours (1972) found that the transition from gamma crystallin to beta and alpha crystallin in *Xenopus laevis* continues through metamorphosis. This lens protein transition might contribute to a change in the refractive index of the lens during metamorphosis. Our raytracing studies on schematic eyes showed that the refractive index of a tadpole lens must be higher than in lenses of toads. The refractive index of the lens in a tadpole eye could change during metamorphosis due to the protein transition and then gradually decline while the lens is growing. That this might be a continuous process is also seen in the difference in calculated values for the refractive indices of lenses in the juvenile toad and the adult toad.

Changes in light sensitivity from the juvenile toad to the adult toad

Our observations with an infrared video camera of toad feeding behavior at different light levels confirm terrestrial observations (Eibl-Eibesfeldt 1967; Taigen and Pough 1981) that young toads tend to be diurnal and adults nocturnal. This lower light sensitivity is also evident in experiments done by Birukow (1950) in which he found just metamorphosed toads (*Bufo calamita*) showed less ability to differentiate brightnesses at low light levels (between 12 and 2 Lux) than adult *Bufo bufo* animals. He interpreted this result as a species specific ability, but we believe the difference in light sensitivity between small and adult toads is a general developmental characteristic in toads and not only limited to the species *Bufo americanus*.

The increased light sensitivity in adult animals cannot be explained totally by the smaller *f*-number of their eyes and their longer red rod outer segments (ROS). The calculated mean *f*-number of 0.85 is consistent with an increase of retinal image brightness by a factor of about 3.5 in adult toads. We can calculate the mean absorption of quanta per photoreceptor from the formula $p = 1-$

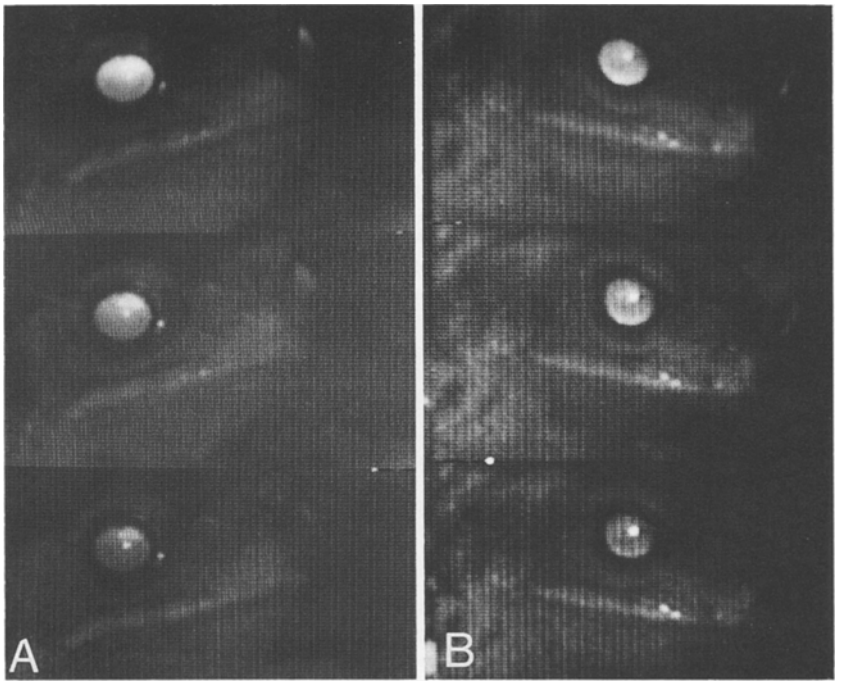

Fig. 10. A Natural accommodation in an adult toad. The resting refractive state in an adult toad is about +8 *D* (hyperopic) as can be calculated from the photoretinoscopic reflex at the top of the pupil. Three subsequent measurements were taken within about 500 ms while IR light sources of increasing eccentricities were flashed into the eyes. **B** The toad fixated a mealworm positioned at a distance of about 5 cm. Note that no hyperopic refraction is observed and that a myopic reflex in the pupil starts to become visible

$10\exp(-kx)$, where $k=0.017$ is the specific absorbance which is assumed to be constant during development (we used the value for the owl) and x is the length of ROS in μm (Martin 1982). The mean quantum capturing probability is 49% in rods of toads in early developmental stages compared to a value of 88% mean absorbance of rods in adult toads. Although the latter value is remarkably high compared to mean absorbances of photoreceptors in other species (owl: 69%, Bowmaker and Martin 1978; pigeon: 71%, Bowmaker 1977; man: 66%, Bowmaker and Dartnall 1980) and although it is almost twice as high as in juvenile toads, it still cannot account fully for the observed light sensitivity.

We did not measure the type and the amount of visual pigment at different developmental stages. Crescitelli (1958) and Muntz and Reuter (1966) showed that the type of visual pigment does not change during development. Toad tadpoles have rhodopsin, which is retained throughout metamorphosis and persists as the adult photopigment. According to Tsukamoto (1987), one can assume that the content of visual pigment is proportional to the ROS volume. We therefore conclude that neuronal parameters must have changed during development and that they are responsible in part for the continuous increase of light sensitivity. Fisher (1972) found changes in retinal synaptic organization in *Rana pipiens* both during maturation and metamorphosis. Although those changes were associated with motion sensitivity, we can expect analogous changes in synaptic formation to improve light sensitivity. Synapse convergence and new synapse formation may increase the gain of the system in this regard. Another mean toads may use to locate prey at low light levels is scent. We consider this possibility unlikely, however, since *Bufo bufo* is also known to be a primarily visually oriented animal that generally does not rely on its sense of smell (von Heusser 1956; Eibl-Eibesfeldt 1967). With our experimental procedure, we evaluated only successful tracking events that were obviously visually guided.

Refractive state and binocular accommodation during feeding behavior in adult toads

Retinoscopic measurements by other authors (Hirschberg 1882; Beer 1898; Krueger and Moser 1971; Millodot 1971, 1974; Moser and Krueger 1972; du Pont and de Groot 1976; Manteuffel et al. 1977) suggest that the resting refractive state of anurans lies within the hyperopic range. In subtracting the measurement artefact for retinoscopy, we find the true resting focus to be nearly emmetropic.

The amount of accommodation we observed (about 8 *D*) is consistent with experiments done by Douglas et al. (1986), who were able to produce binocular accommodation of about 10 *D* by applying drugs (miotic and atropine) to toad eyes (in

Bufo viridis). At the same time, they observed an accompanying shift in lens position of about 150 μm (by taking photographs of the eye from above) while apparently there was no change in curvature of either the anterior lens surface or the cornea. They calculated that a shift in lens position of 150 μm was not enough to achieve this amount of accommodation. Calculations based on our schematic eye show that a lens movement of about 200 μm is theoretically necessary to produce 8 *D* of accommodation. Douglas et al. (1986) suggested that alterations of the axial length together with a shift in lens position both play a role in altering the refractive state of toad eyes. The retinoscopic measurements during feeding behavior showed that the optical quality of the eye deteriorates during accommodation. However, a significant, clearly visible increase of aberration is only produced by changing the outer radii of curvature of the lens and not by altering the position of the lens or the axial length of the eye. Since Douglas et al. (1986) stated that there is no change in curvature of either the cornea or the anterior lens surface during accommodation, one could assume that the radius of curvature of the posterior lens surface decreases during accommodation, thereby increasing the refractive power of the eye. The range of accommodation as measured with photoretinoscopy did not extend beyond 8 *D* (corresponding near point for an emmetropic eye: 0.15 m). The prey object was closer than 15 cm when accommodation occurred. This might lead to the conclusion that the animal did not focus perfectly on the prey. However, for an eye of comparably low optical resolution but high light sensitivity, a considerable amount of depth of focus is present. Therefore, the optical resolution may have already been at its optimum for the given amount of accommodation and further improvement would not occur.

Our experiments showed that accommodation was not essential for a binocular toad to catch the prey because we observed successful snapping events without previous accommodation. Usually accommodation was observed during the short cessation of locomotion just prior to the snapping event. This is consistent with studies on prey capture behavior in salamanders done by Werner and Himstedt (1984). They found a myopic shift in refraction before the animal turned to the prey. The pause just prior to snapping is an indispensable link in the stereotypical behavior pattern of feeding in toads. It has been described by several authors (Eibl-Eibesfeldt 1967; Eikmanns 1955), and Hinsche (1935) called it T-phenomenon or reflex-delay (Reflex-Verspätung). It might be possible that, by using the accommodative cue during this pause, the toad wants to verify visually whether the prey is worth snapping at or not.

Acknowledgements. We thank Dr. H. Pough for calling our attention to the shift in activity from diurnal to nocturnal vision during the development of toads. We also acknowledge the skillful programming help of Dr. C.-H. Wenninger and A. Glasser. We thank Mrs. L. Peck and two anonymous referees for their many helpful suggestions regarding this manuscript. This work was supported by NIH grant EY-02994 to H.C. Howland.

References

Beer T (1898) Die Akkommodation des Auges bei den Amphibien. Pflügers Arch Ges Physiol 73:501–534

Birukow G (1950) Vergleichende Untersuchungen über das Helligkeits- und Farbensehen bei Amphibien. Z Vergl Physiol 32:348–382

Bowmaker JK (1977) The visual pigments, oil droplets and spectral sensitivity of the pigeon. Vision Res 17:1129–1138

Bowmaker JK, Dartnall HJA (1980) Visual pigments of rods and cones in a human retina. J Physiol (Lond) 298:501–511

Bowmaker JK, Martin GR (1978) Visual pigments and colour vision in a nocturnal bird, *Strix aluco* (Tawny owl). Vision Res 18:1125–1130

Brahma SK, Bours J (1972) Thin layer isoelectric focusing of the soluble lens extracts from larval stages and adult *Xenopus laevis*. Exp Eye Res 13:309–314

Collett TS (1977) Stereopsis in toads. Nature 267:349–351

Crescitelli F (1958) The natural history of visual pigments. In: Newburgh RW (ed) Photobiology, Biology Colloquium, Oregon State College, Corvallis, pp 30–51

Davson H (1984) Vegetative physiology and biochemistry. vol IA In: Davson H (ed) The eye. Academic Press, London

Douglas RH, Collett TS, Wagner HJ (1986) Accommodation in anuran Amphibia and its role in depth vision. J Comp Physiol A 158:133–143

Doyle MJ, Maclean N (1978) Biochemical changes in developmentally retarded *Xenopus laevis*. I. The lens crystallin transition. J Embryol Exp Morphol 46:215–255

Duke-Elder S (1958) The eye in evolution. (System of ophthalmology. vol I) Henry Kimpton, London

Eibl-Eibesfeldt I (1967) Nahrungserwerb und Beuteschema der Erdkröte. Behavior 4:1–35

Eikmanns KH (1955) Verhaltensphysiologische Untersuchungen über den Beutefang und das Bewegungssehen der Erdkröte (*Bufo bufo* L.). Z Tierpsych 12:229–253

Fisher LF (1972) Changes during maturation and metamorphosis in the synaptic organization of the tadpole retina inner plexiform layer. Nature 235:391–393

Glickstein M, Millodot M (1970) Retinoscopy and eye size. Science 168:605–606

Gordon J, Hood DC (1976) Anatomy and physiology of the frog retina. In: Fite K (ed) The amphibian visual system. Academic Press, New York, pp 29–86

Hess C von (1911) Beiträge zur vergleichenden Akkommodationslehre. Zool Jahrb 30:339–359

Heusser H von (1956) Zum geruchlichen Beutefinden und Gähnen der Kreuzkröte (*Bufo calamita* Laur.). Z Tierpsychol 15:94–98

Hinsche G (1935) Ein Schnappreflex nach Nichts bei Anuren. Zool Anz 3:113–122

Hirschberg I (1882) Zur Dioptrik und Ophthalmoskopie der

Fisch- und Amphibienaugen. Arch Anat Physiol Abt Physiol 1882:493–526
Howland HC (1985) Optics of photoretinoscopy: results from raytracing. Am J Optom Physiol Opt 62:614–620
Ingle DJ (1968) Visual releasers of prey catching behavior in frogs and toads. Brain Behav Evol I:500–518
Ingle DJ (1976) Spatial vision in anurans. In: Fite K (ed) The amphibian visual system. Academic Press, New York, pp 119–149
Jordan M, Luthardt G, Meyer-Naujoks Chr, Roth G (1980) The role of eye accommodation in the depth perception of common toads. Z Naturforsch 35c:851–852
Koneff (1938) Mallory Heidenhain's azan stain. In: Humason GL (ed) Animal tissue techniques. Freeman and Company, San Francisco, pp 163–165
Krüger H, Moser EA (1971) Refraktion und Abbildungsgesetze des Froschauges. Pflügers Arch 326:334–852
Larsen LO, Pedersen JN (1982) The snapping response of the toad, *Bufo bufo*, towards prey dummies at very low light intensities. Amph Rept 2:321–327
Manteuffel G, Wess O, Himstedt W (1977) Measurements of the dioptric apparatus in amphibian eyes and calculations of the visual acuity in water and in air. Zool Jb Physiol 81:395–406
Martin GR (1982) An owl's eye: schematic optics and visual performance in *Strix aluco* L. J Comp Physiol 145:341–349
Millodot M (1971) Measurement of the refractive state of the eye in frogs (*Rana pipiens*). Rev Can Biol 30:249–252
Millodot M (1974) Optical measurement of the refraction of the eyes in frogs (*Rana pipiens*). Pflügers Arch 351:173–175
Moser EA, Krüger H (1972) Retinoscopic and neurophysiological refractometry in *Rana temporaria*. Pflügers Arch 335:235–242
Muntz WRA, Reuter T (1966) Visual pigments and spectral sensitivity in *Rana temporaria* and other European tadpoles. Vision Res 6:601–618
Pont JS du, de Groot PJ (1976) A schematic dioptric apparatus for the frog's eye (*Rana esculenta*). Vision Res 16:803–810
Schaeffel F, Howland HC (1987) Corneal accommodation in chick and pigeon. J Comp Physiol A 160:375–384
Sivak JG, Warburg MR (1980) Optical metamorphosis of the eye of *Salamandra salamandra*. Can J Zool 58:2059–2064
Taigen TL, Pough FH (1981) Activity metabolism of the toad (*Bufo americanus*): ecological consequenes of ontogenetic change. J Comp Physiol 144:247–252
Tretjakoff D (1913) Zur Anatomie des Auges der Kröte. Z Wiss Zool 80:327–359
Tsukamoto Y (1987) Morphometrical features of rod outer segments in relation to visual acuity and sensitivity in the retina of *Rana catesbeiana*. Zool Sci 4:233–242
Walls GL (1942) The vertebrate eye and its adaptive radiation. Hafner Publishing Co., New York, London
Werner C, Himstedt W (1984) Eye accommodation during prey capture behavior in salamanders (*Salamandra salamandra* L.). Behav Brain Res 12:69–73